31st Annual International Conference of the IEEE EMBS
Minneapolis, Minnesota, USA, September 2-6, 2009

Optimal tissue types in the thoracic electrical impedance model for thoracic electrical bioimpedance (TEB) studies

M. Akhand[1], A. Trakic[1], P. Terril[1], F. Liu[1], S. Wilson[1] and S. Crozier[1]

Abstract— **In this study we have identified the tissues required to be included in the thoracic electrical impedance model for studies relating to impedance cardiography. This is a useful finding, as it expedites and simplifies the segmentation process when employed to construct digital human models from a set of magnetic resonance or computed tomography images. Laplace equations with inhomogeneous boundary conditions were solved within an anatomically accurate thorax model. When the number of tissue types in the model was reduced to only 7 (i.e. blood, fat, liver, lung, muscle, skin and bone) the calculations indicated a 3.6% error in the result. Addition of internal air reduced the error to as small as 1.3%. Further reductions in the number of tissue types introduced larger errors in the measurement. It was therefore concluded that 8 tissue types are essential to acceptably preserve the computational accuracy while facilitating a simplification of the segmentation process.**

I. Introduction

Thoracic electrical bioimpedance (TEB) is a non-invasive technique which utilizes the pulsatile changes of thoracic impedance with the ventricular systole and diastole to calculate the stroke volume (SV). (SV = end diastolic volume – end systolic volume). Measurement of cardiac output is crucial for critically ill patients and monitoring the affect of therapeutic maneuvers [1]. Two categories of methods for measuring cardiac output exist namely, invasive and noninvasive. All the invasive methods requires entrance into the body for the purpose of inserting a catheter, withdraw blood or exposing a vessel [2]. Noninvasive method can calculate the cardiac output without any invasion into the body. Various methods which are relatively non-invasive to the palmonary artery catheters exists namely, oesophageal doppler ultrasonography, transoesophageal echocardiography, lithium dilution cardiac output and pulse pressure analysis techniques [3]. TEB is a non-invasive technique which if appropriately applied, is a very effective means of evaluating the cardiac output (CO). In TEB, two or more electrodes are commonly placed on the chest (and neck) to induce electric currents within the chest [5]. The magnitude and path of the induced currents are modified by different electrical impedances of thoracic tissues, causing a non-uniform voltage potential field on the surface and inside the torso. The same or additional electrodes are then used to measure the difference in voltage potentials [4],[5]. According to Kirchhoff's law electric current passes through the path of least resistance or higher conductance. In the body blood and plasma has the lowest resistivity which makes the induced current distributes through blood and extracellular fluid. Blood volume change with cardiac cycle alters the resistance of the whole body. As a result SV is associated with the proportional increase in the measurable conductance of the whole body [6],[7]. The SV can be calculated using Kubicek [8],[9], Sramek [6] or Tischenko [10],[11] algorithm from the impedance cardiogram constructed from the recorded potential on the body surface. Being a non-invasive method TEB eliminates the risks of invasive methods [2].

In-vivo TEB provides us with a good estimate of the SV. A thoracic model created by segmenting magnetic resonance images (MRI) of a patient provides us with a non-invasive means of measuring the blood volume inside the heart during the cardiac cycle. The thoracic model enables the calculation of the end systolic/diastolic blood volume and the SV. Numerical simulation calculates the potential differences on the body surface and TEB algorithm calculates the SV. The comparison of these two SVs will enable us to optimize the TEB measure of CO.

Since TEB measure of CO uses impedance cardiogram, which results from the blood volume change in the heart, the thorax model must be electrically correct. Tissue impedances play a crucial role in the thorax model as a volume conductor [13]. In order to calculate the body surface potential due to the change in blood volume, it is necessary to construct a thoracic model that accurately represents the conductive properties of different tissue types Identification of all the tissue types in MR images becomes difficult due to resolution and noise. Segmentation of a set of MR images is a time consuming process and there is no existing software package that accomplishes the task automatically with the required perfection. Manual and semi-automatic segmentation are often the only available methods. The complexity and the time required for segmentation increases with the number of target tissue types. Therefore, proper identification and segmentation of a large number of tissue types present in MR images can be extremely tedious and difficult. To expedite and simplify the segmentation process and at the same time to obtain accurate impedance cardiogram, it is important to identify and segment only those tissues which largely contribute to the difference in electrical potentials at the cost of a small, yet acceptable deviation in the potential difference.

In this study, we have conducted a number of computer simulations to identify the eight dominant thoracic tissues that strongly contribute to the surface potential differences due to the change in blood volume.

[1] The School of Information Technology and Electrical Engineering, The University of Queensland, St. Lucia, Brisbane, Queensland 4072, Australia.

II. METHODS

A. Numerical methods

The numerical solution of the forward problem requires the solution of the Laplace's equation

$$\nabla \cdot (\sigma \nabla)\varphi = 0 \qquad (1)$$

With the inhomogeneous boundary conditions [14], [15], [16].

$$\sigma \frac{\partial \varphi}{\partial n} = J \qquad (2)$$

where φ is the potential, σ is the inhomogeneous conductivity of the medium and

$$J = \frac{I_l}{|e_l|} \quad on\ e_l, l = 1,2,\dots,L$$

$$J = 0 \quad off \bigcup_{l=1}^{L} e_l$$

Where $|e_l|$ denotes the area (in m^2) of the electrode surface, I denotes the injected current (in Amps), J denotes the current density, and l denotes the number of electrodes. We solve the forward problem with the following two additional conditions

Conservation of charge: $\sum_{l=1}^{L} I_l = 0$
Choice of ground: $\sum_{l=1}^{L} \varphi_l = 0$

We divide the computational space into a large number of cubes and approximate the solution of the Laplace's equation for each cubic cell. The solution of the Laplace's equation in the $(i,j,k)^{th}$ cell is obtained as follows

$$\varphi_{i,j,k} = \frac{\sum_{m=0}^{1}(\varphi_{i+m,j,k}\sigma^a_{i+m,j,k} + \varphi_{i,j+m,k}\sigma^a_{i,j+m,k} + \varphi_{i,j,k+m}\sigma^a_{i,j,k+m})}{\sum_{m=0}^{1}(\sigma^a_{i+m,j,k} + \sigma^a_{i,j+m,k} + \sigma^a_{i,j,k+m})} \qquad (3)$$

The governing equation in finite-difference form (3) is solved iteratively using Successive Over Relaxation (SOR) algorithm [17]. The method has been validated in [18],[19]. Here σ^a is the conductivity of the interface. Each cube has six interfaces and therefore six interface conductivities. These six interface conductivities are indexed as $(\sigma^a_i, \sigma^a_{i+1})$, $(\sigma^a_j, \sigma^a_{j+1})$, $(\sigma^a_k, \sigma^a_{k+1})$ along the x, y and z axis respectively. The electric potential is calculated at the centre of the cube hence there is one electric potential value for each cube. The conductivity at the interface σ^a is calculated as the harmonic average of the conductivities of the two adjacent cubes σ_c and σ_b [20].

$$\sigma^a = \frac{2\sigma_c\sigma_b}{\sigma_c + \sigma_b} \qquad (4)$$

B. The Thorax model

Brook's body model is a generic electrical model of human body which contains the conductivity (or alternatively impedance) values of different tissue types. We have separated the thorax from the whole body model with the height of 160 voxels (from 120 to 280) and the width of 179 voxels (from 57 to 236), where each voxel is a cube of 8 mm^3. Thorax model is shown in Figure 1(12).

Brook's body model contains the tissue type conductivity values in voxels. We can merge two or more tissue types into one tissue type by assigning the same tissue type conductivity to the corresponding voxels. In this way it is possible to construct a thoracic model that contains a small number of tissue types. Cross sections of the thorax model with different combinations of tissues are shown in Figure 2. Our aim is to include the minimum number of tissue types while representing the maximum conductivity information within the model. If we want to approach the blood inside the heart from the chest surface we will encounter layers of skin, fat, muscle, bone and heart muscle. The heart sits between the Liver and lung and they occupy a large area inside the thorax.

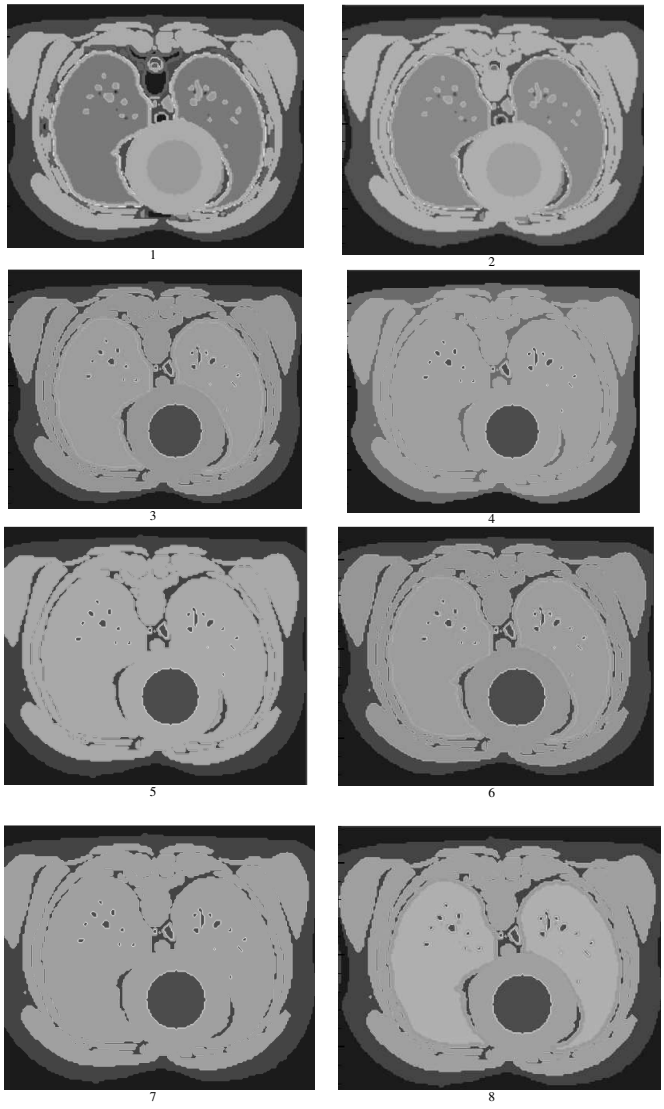

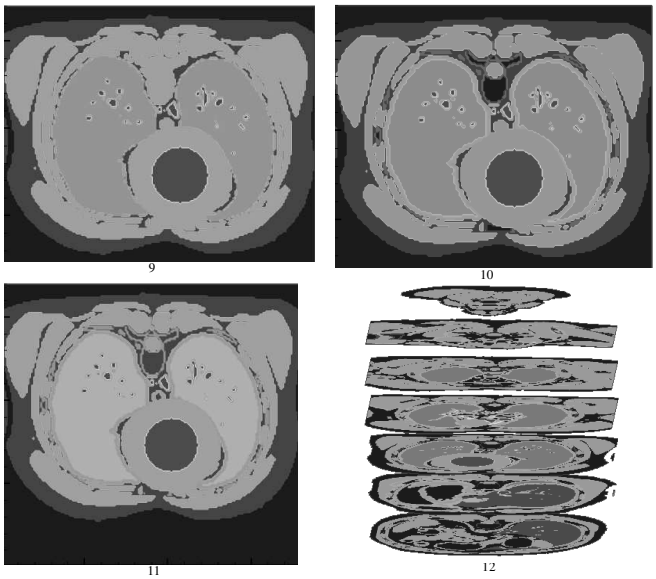

Fig 1. Cross section of the thorax with the spherical heart and different combinations of tissue types (1) All tissues (2) All tissues with bone merged with the muscle (3) blood, fat, liver, lung, muscle skin (4) blood, fat, liver, lung, muscle, skin, bile, gall bladder (5) blood, fat, muscle, skin (6) blood, fat, lung, muscle, skin (liver merged with muscle) (7) blood, fat, liver, muscle, skin (lung merged with muscle) (8) blood, fat, lung, muscle, skin (liver merged with lung) (9) blood, fat, lung, muscle, skin (lung merged with liver) (10) blood, fat, liver, lung, muscle, skin, bone (11) blood, fat, liver, lung, muscle, skin , bone ,internal air (12) The Thorax model with spherical heart

Considering the anatomical structure of the thorax inclusion of these tissue types in the model is crucial. Besides, muscle, fat, lung, liver, bone, skin, blood and internal air contribute significantly towards the total volume of the thorax. Different tissue types and their volumes are shown in Table I. For purposes of this initial study, replacing the heart inside the Brook's body model with a sphere of varying size, is one straight forward means of modelling diastolic and systolic states of the heart. We replace the heart inside the thorax with a sphere in such a way that the distance from the surface of the chest to the sphere wall touching the ribcage is the same as that with the real heart. The sphere has a wall which is assigned the conductivity of muscle and it contains blood inside. The spherical heart model is assumed to initially represent the diastolic state of the heart. In order to create similar structure of the systolic state we have increased the thickness of the wall and reduced the blood volume inside the sphere. Now, we effectively have two thorax models, the first one contains the *diastolic heart* and the second one contains the *systolic heart*.

Table I

Cumulative volume and tissue conductivities in the thorax model

Tissue types	Volume (%)	Conductivity* (S/m)
Muscle	34.41	0.35
Fat	26.26	0.024
Lung	14.08	
Lung inner		0.1
Lung outer		0.26
Liver	5.80	0.065
Bone	4.92	
Bone cancellous		0.083
Bone cortical		0.021
Bone marrow		0.003
Skin	3.55	0.00023
Blood	3.13	0.70
Internal air	1.71	0.00012
Heart	1.26	0.18
Cartilage	0.90	0.18
Blood vessel	0.72	0.32
Spleen	0.71	0.12
Stomach	0.55	0.53
Ligaments	0.40	0.39
Nerve spine	0.32	0.061
Mucous membrane	0.32	0.0014
Intestine	0.27	0.57
Glands	0.16	0.53
CSF	0.14	2.0
Pancreas	0.13	0.53
Lymph	0.12	0.53
Bile	0.04	1.40
Gall bladder	0.02	0.9

*[12],[21]

C. *Electrode interface with the thorax model*

We have placed two electrodes on the chest surface of the model where each electrode surface area (1 cm^2) is in contact with the body surface. The centres of the two electrodes are at voxel (121, 27, 105) and (76, 30, 105). In addition, effective electrical conductivities of 4.6e-4 S/m were assigned to the two electrode models. The effective conductivity is calculated as the harmonic average of the conductivities of the silver electrode and the skin by using equation (4).

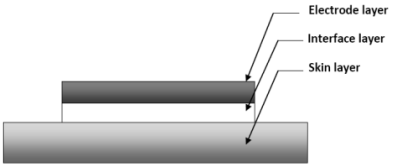

Fig 2. Electrode interface

Table II

Potential differences for stroke volume (SV) and errors introduced in the measurement for considering different combinations of tissue types

Tissue types	Potential difference (mV) due to SV	Error *(%)
All	78.6	
All with bone merged with muscle	62.2	20.87
Blood, fat, liver, lung, muscle and skin	60.4	23.16
Blood, fat, liver, lung, muscle, skin, bile and gall bladder	53.3	32.19
Blood, fat, liver, lung, muscle, skin and bone	75.8	3.56
Blood, fat, liver, lung, muscle, skin, bone and internal air	79.6	1.27
Blood, fat, muscle and skin	53.3	32.19
Blood, fat, lung, muscle, skin (Liver merged with muscle)	56.8	27.74
Blood, fat, liver, muscle, skin (Lung merged with muscle)	56.9	27.61
Blood, fat, lung, muscle, skin (liver merged with lung)	57.5	26.84
Blood, fat, lung, muscle, skin (lung merged with liver)	58.2	25.95

*Error calculated as a percentage of potential difference for all tissue types

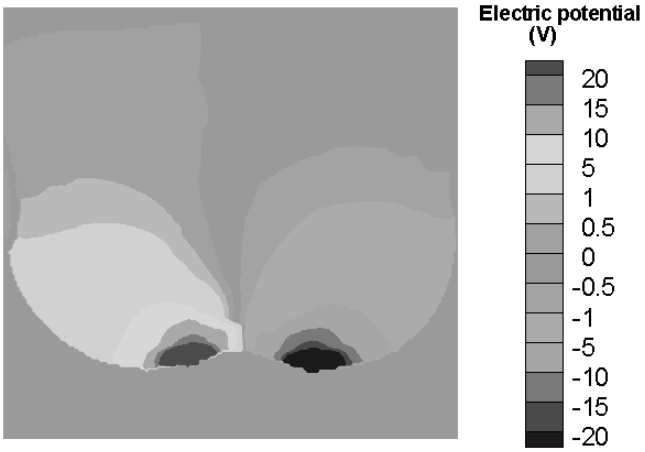

Fig 3. Cross section of the thorax with electric potential.

III. RESULTS

The forward problem was solved with different sets of tissue types (see Figure 1) and systolic/diastolic spherical heart. Electric potential inside the thorax due to the current injection is shown in Figure 3. The simulation results for the recorded potential differences due to the stroke volume of 103.2 ml (End Systolic Volume 33.4 ml and End Diastolic Volume 136.6 ml) and the errors are shown in Table II.

IV. DISCUSSION

With all the tissue types the recorded potential difference for the SV of 103.2 ml is 78.6 mV. We consider this measured value of the potential as the optimum and compare other measured value of the potential to it. Reduction in the number of tissue types to seven (i.e. Blood, fat, liver, lung, muscle, skin and bone) underestimates the measurement by 3.6%. Also, exclusion of bone tissues from this seven dominant tissue types increases the underestimate to 23%. However, the inclusion of internal air reduces the error by over estimating the electric potential by 1.3%. An effort to reduce the number of tissue types further by merging lung, liver and muscle produces larger error in potential measurement.

ACKNOWLEDGMENT

This work was supported by the School Shared (ITEE/Research Grant) Scholarship, School of Information Technology and Electrical Engineering, The University of Queensland.

REFERENCES

[1]. Jing P Sun, Min Pu, Fetnat M. Fouad, et al., "Automated Cardiac Output Measurement by Spatiotemporal Integration of Color Doppler Data: In Vitro and Clinical Validation," Circulation, vol.95, pp.932-939, 1997.

[2]. Kevin C. Ehlers, Kenneth C. Mylrea, Charles K. Waterson, Jerry M. Calkins, "Cardiac output measurements. a review of current techniques and research," Annals of Biomedical Engineering, vol.14, pp.219-239, 1986.

[3]. D.A. Hett and M.M. Jonas, "Non-invasive cardiac output monitoring,"Current Anaesthesia & Critical Care, vol.14, pp.187-191, 2003

[4]. R. P. Patterson, "Fundamentals of impedance cardiography," IEEE Engineering in Medicine and Biology Magazine, pp. 35-38, 1989.

[5]. J. Verdu, "Electrical impedance method for the measurement of stroke volume in man: state of art," Acta et Comm., Uni. Tartuensis, Jartu, Estonia, 1994.

[6]. Sramek B B, Rose D M, and Miyamoto A, "A stroke volume equation with a linear base impedance model and its accuracy as compared to thermodilution and magnetic flow techniques in humans and animals," in *Proc. Proceedings of the Sixth International Conference on Electrical Bioimpedance,* Zadar, Yugoslavia, pp. 38, 1983

[7]. Djordjevich L, Sadove MS, "Basic principles of electrohaemodynamics," J Biomed Eng, vol.3, pp.25–33, 1981

[8]. Kubicek WG, Karnegis JN, Patterson RP, et al., " Development and evaluation of an impedance cardial output system," Aerospace Med, vol.37, pp. 1208-1212, 1966

[9]. Kubicek WG, Patterson RP, and Witsoe DA, "Impedance cardiography as a noninvasive method of monitoring cardiac function and other parameters of the cardiovascular system," Ann. N.Y. Acad. Sci., no. 170, pp. 724-732, 1970.

[10]. Tischenko MI, "Estimation of the stroke volume by integral rheogram of the human body. (in Russian)," Fiziol. Zhurnal SSSR, vol.59, pp. 1216-1224, 1973.

[11]. Tischenko MI, Smirnov AD, Danilov LN, and Alexandrov AL, "The characteristics and clinical use of integral rheography - a new method for measuring stroke volume. (in Russian)," Kardiologija (Moscow) vol.13, pp. 54-62, 1973.

[12]. S.Gabriel, R.W.Lau and C.Gabriel, "The dielectric properties of biological tissues: II. Measurements in the frequency range 10 Hz to 20 GHz," Phys. Med. Biol., vol.41, pp.2251-2269, 1996

[13]. Jari Hyttinen, Pasi Kauppinen, Tiit Koobi, and Jaakko Malmivuo, "Importance of the tissue conductivity values in modeling the thorax as a volume conductor," in *Proc. 19th International Conference - IEEE/EMBS* (Chicago, IL. USA), pp. 2082-2085, 1997.

[14]. Johan Andoyo Effend Noor, "Electrical impedance tomography at low frequencies," Ph.D. dissertation, University of New South Wales, 2007.

[15]. Erkki Somersalo, Margaret Cheney, and David Isaacson, "Existence and uniqueness for electrode models for electric current computed tomography", SIAM Journal on Applied Mathematics, vol.52, no. 4, pp. 1023-1040, 1992.

[16]. Guizhi Xu, Huanli Mu, Shuo Yang, et al., "3-D electrical impedance tomography forward problem with finite element method," IEEE Transactions on Magnatics, vol.41, pp. 1832-1835, 2005.

[17]. Feng Liu, Huawei Zhao, and Stuart Crozier, "On the Induced Electric Field Gradients in the Human Body for Magnetic Stimulation by Gradient Coils in MRI," IEEE Transactions on Biomedical Engineering, vol. 50, no. 7, pp. 804-815, 2003.

[18]. Liu F, Crozier S, Zhao HW and Lawrence B, "Finite-difference time-domain-based studies of MRI pulsed field gradient-induced eddy currents inside the human body," Concepts inMagn.Reson.vol.15, pp.26-36, 2002.

[19]. Liu F and Crozier S, "Electromagnetic fields inside a lossy, multilayered spherical head phantom excited by MRI coils," models and methods Physics in Medicine and Biology, vol.49, pp.1835-51, 2004.

[20]. J. G. Witwer, G. J. Trezek, and D. L. Jewett, "The effect of media in homogeneities upon intracranial electrical fields,"IEEE Trans. Biomed.Eng. vol.BME-19, no.5, pp. 352-362, 1972.

[21]. Gabriel C, Gabriel S and Corthout E, "The dielectric properties of biological tissues: I. Literature survey," Physics in Medicine and Biology, vol.41, pp.2231–49, 1996.